# Correspondence normalized ghost imaging on compressive sensing*

Zhao Sheng-Mei(赵生妹)† and Zhuang Peng(庄 鹏)

*Institute of Signal Processing & Transmission, Nanjing University of Posts and Telecommunications, Nanjing* 210003, *China*

(Received 21 August 2013; revised manuscript received 22 October 2013; published online 25 March 2014)

Ghost imaging (GI) offers great potential with respect to conventional imaging techniques. It is an open problem in GI systems that a long acquisition time is be required for reconstructing images with good visibility and signal-to-noise ratios (SNRs). In this paper, we propose a new scheme to get good performance with a shorter construction time. We call it correspondence normalized ghost imaging based on compressive sensing (CCNGI). In the scheme, we enhance the signal-to-noise performance by normalizing the reference beam intensity to eliminate the noise caused by laser power fluctuations, and reduce the reconstruction time by using both compressive sensing (CS) and time-correspondence imaging (CI) techniques. It is shown that the qualities of the images have been improved and the reconstruction time has been reduced using CCNGI scheme. For the two-grayscale "double-slit" image, the mean square error (MSE) by GI and the normalized GI (NGI) schemes with the measurement number of 5000 are 0.237 and 0.164, respectively, and that is 0.021 by CCNGI scheme with 2500 measurements. For the eight-grayscale "lena" object, the peak signal-to-noise rates (PSNRs) are 10.506 and 13.098, respectively using GI and NGI schemes while the value turns to 16.198 using CCNGI scheme. The results also show that a high-fidelity GI reconstruction has been achieved using only 44% of the number of measurements corresponding to the Nyquist limit for the two-grayscale "double-slit" object. The qualities of the reconstructed images using CCNGI are almost the same as those from GI via sparsity constraints (GISC) with a shorter reconstruction time.

**Keywords:** ghost imaging, compressive sensing, time-correspondence, normalizing

**PACS:** 42.50.Ar, 42.30.Wb, 42.25.Kb, 42.30.Va **DOI:** 10.1088/1674-1056/23/5/054203

## 1. Introduction

Ghost imaging (GI), also called coincidence imaging or correlated imaging, has attracted much attention recently.[1–10] In a GI system, the image of an object is retrieved by using two spatially correlated beams, a signal beam and a reference beam. The signal beam after illuminating an object is collected with a bucket detector with no spatial resolution. The reference beam never interacts with the object and is detected by a pixel-related detector. By correlating the reference beam with the bucket signal, the "ghost image" will be recovered in the reference beam.

The first GI scheme was proposed by Klyshko in 1980s,[1] which was based on the entangled-photon pairs generated by spontaneous parametric down-conversion (SPDC). Later, it was shown and demonstrated that GI could be realized with classical light sources,[8–35] especially pseudo-thermal sources. Both entangled sources and thermal lights can be used to realize GI, but thermal lights are more attainable in comparison with quantum entanglement photon pairs.

It is an open problem in GI systems that a long acquisition time is be required for reconstructing images with good visibility and signal-to-noise ratio (SNR). To improve the quality of the reconstructed image in the GI system, Gong *et al.* proposed a method based on the correlation measurement of intensity fluctuations in time–space-average domain to improve the visibility of ghost images.[14] Later, Ferri *et al.* presented a differential ghost imaging (DGI) scheme to greatly enhance the SNR of imaging.[15] Similarly, Sun *et al.* proposed a normalized ghost imaging (NGI) to obtain a higher quality of the imaging via eliminating the noise caused by laser power fluctuations.[16] It had shown that the SNR performance of the NGI scheme was matched to that of DGI scheme.[16] In addition, a new imaging approach called ghost imaging via sparsity constraints (GISC) was shown to be able to reconstruct pseudo-thermal GI with high quality.[17]

Simultaneously, two methods have been developed to reduce the reconstruction time in a GI system. One method uses a compressive sensing (CS) technique.[37,38] For example, Katz *et al.* proposed a compressive GI scheme, which reduced the required acquisition time significantly.[18] Han *et al.* presented some effective GI schemes with compressive sensing,[19–24] and we gave a differential compressive correlated imaging with a shorter reconstruction time.[25] The other methods use the time-correspondence technique.[26–28] For instance, Luo *et al.* presented a time-correspondence imaging (CI) scheme to decrease the reconstruction data to the half of normal reconstruction measurements.[26,27]

In this paper, we present a novel GI scheme by integrating the normalizing technique, the CS technique, and the CI technique. In the scheme, we enhance the SNR performance by normalizing the reference beam intensity to eliminate the

*Project supported by the National Natural Science Foundation of China (Grant No. 61271238), the Specialized Research Fund for the Doctoral Program of Higher Education of China (Grant No. 20123223110003), and the University Natural Science Research Foundation of Jiangsu Province, China (Grant No. 11KJA510002).

†Corresponding author. E-mail: zhaosm@njupt.edu.cn

© 2014 Chinese Physical Society and IOP Publishing Ltd 

noise caused by laser power fluctuations, and reduce the reconstructing time by using both CS and CI techniques. We name it the correspondence normalized ghost imagining based on compressive sensing (CCNGI) scheme. It is shown that the image qualities have been improved and the reconstruction time has been reduced. The CCNGI is a scheme with a short reconstructing time and a good signal-to-noise ratio.

## 2. Correspondence normalized GI based on compressive sensing

In this section, we present the CCNGI scheme and the theoretical analysis of the performance of the scheme. We first give the CCNGI scheme.

The schematic diagram of CCNGI scheme is shown in Fig. 1. CCNGI scheme is a lensless GI system with pseudo-thermal light. The pseudo-thermal light is divided into two spatially correlated beams by a 50:50 beam splitter (BS), the signal beam (SIG), and the reference beam (REF). The signal beam illuminates the object at distance $z_1$ from the source, and the bucket signal is collected with a bucket detector, where $S_i$ denotes the measurement value of the $i$-th observation of the bucket detector. The reference beam is detected by a CCD with distance $z_2$. Here, $z_1 = z_2$ is assumed, $I_i(x,y)$ indicates the light intensity distribution of the $i$-th measurement from CCD, $R_i$ is obtained by summarizing the light intensity distribution $I_i(x,y)$ at the reference beam, and $S_i$ is normalized to $S'_i$, where $S'_i = S_i/R_i$, $\langle S' \rangle$ is defined as an ensemble average from $M$ measurements of $S'_i$.

For convenience, we also present the schematic diagram of a traditional GI scheme and a normalized GI system in Fig. 1. The components with a black dashed line represent the traditional GI scheme, the red dashed one indicates the normalized GI scheme, and the solid line is our proposed scheme.

In the CCNGI scheme, we utilize the CI technique to choose the measurement data for compressive sensing. Here, we choose the measurement data $S'^{+}_i$ to compose the measurement vectors $\{S'^{+}_i\}$ in a compressive sensing algorithm, where $\{S'^{+}_i\}$ are those measurements data which are greater than the ensemble average $\langle S' \rangle$ in the signal beam. At the same time, we select the corresponding measurements data $\{I_i(x,y)^+\}$ in the reference beam as the measurement matrix in compressive sensing algorithm. For each $I_i(x,y)^+$, $i = 1,\ldots,M$, $x,y = 1,\ldots,n$, the matrix formula of the light intensity distribution of all pixels on CCD is

$$\boldsymbol{I}_i^+ = \begin{bmatrix} I^i_{11} & \cdots & I^i_{1n} \\ \vdots & \ddots & \vdots \\ I^i_{n1} & \cdots & I^i_{nn} \end{bmatrix}, \tag{1}$$

where $\boldsymbol{I}_i^+ = [I_i(x,y)^+]$, $I^i_{mn} = I_i(x = m, y = n)^+$. It can be reformed to a one-dimensional vector $\boldsymbol{I}_i^+ = [I^i_{11}, I^i_{12}, \ldots, I^i_{1n}, I^i_{21}, I^i_{22}, \ldots, I^i_{n,n-1}, I^i_{nn}]$. Using CI technique to choose the measurements data, we only need select some of the light intensity distributions $\{I_i(x,y)^+\}$ corresponding to $\{S'^{+}_i\}$ as the measurement matrix in CCNGI. For example, $p$ measurements are enough. It was shown that the measurements data using the CI technique are approximately the half of that in the traditional GI scheme.[27,28] Hence, the measurement number $p$ is at most equal to the half traditional measurement numbers, that is $p \le M/2$. Finally, the measurement matrix for compressive sensing is

$$\begin{bmatrix} \boldsymbol{I}_1^+ \\ \boldsymbol{I}_2^+ \\ \vdots \\ \boldsymbol{I}_p^+ \end{bmatrix} = \begin{bmatrix} I^1_{11} & \cdots & I^1_{1n} & \cdots & I^1_{nn} \\ I^2_{11} & \vdots & \ddots & & I^2_{nn} \\ \vdots & \vdots & & \ddots & \vdots \\ I^p_{11} & \cdots & I^p_{1n} & \cdots & I^p_{nn} \end{bmatrix}. \tag{2}$$

It is a matrix with size of $p \times n^2$, where each row denotes the light intensity distribution for one measurement in the reference beam, and each column represents $p$ light intensity values at position $(x,y)$. Simultaneously, the corresponding measurement vector is composed by $S'^{+}_i$ with size of $p \times 1$. According to the correlated imaging theory, $S'^{+}_i$ is the $i$-th normalized observation value in the signal bucket detector, for $\int I_i^+(x,y)\,\mathrm{d}x\mathrm{d}y$ is approximately a constant for each observation

$$\begin{aligned} S'^{+}_i &= \frac{\int I_i^+(x,y)T(x,y)\,\mathrm{d}x\mathrm{d}y}{\int I_i^+(x,y)\,\mathrm{d}x\mathrm{d}y} \\ &\approx C_0 \int I_i^+(x,y)T(x,y)\,\mathrm{d}x\mathrm{d}y, \quad (i = 1,\ldots,M), \end{aligned} \tag{3}$$

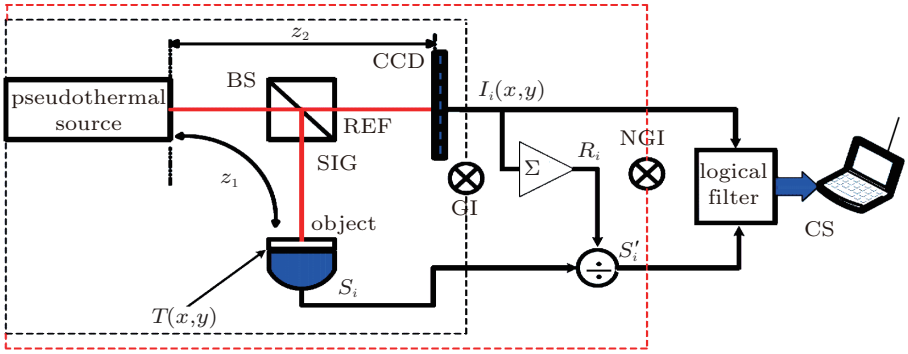



**Fig. 1.** (color online) Schematic diagram of the experimental setup.

Here, we note that the vectors $\{I_i(x,y)^+\}$ are random and most likely linearly independent. In addition, natural images are sparse for most imaging tasks. That is, they contain many coefficients close to or equal to zero when represented in an appropriate basis (e.g., the discrete cosine transform, DCT). We could apply the CS recovery algorithm to Eq. (3). It requires solving the convex optimization program, for seeking for the image $T_{\rm CS}$ which minimizes the $l_0$-norm in the sparsity basis

$$T_{\rm CS} = T(x,y) : \arg\min \|\Psi T(x,y)\|_{l_0}$$

subject to

$$S'^{+}_i \propto \int I_i(x,y)^+ T(x,y)\,{\rm d}x{\rm d}y, \tag{4}$$

where $T_{\rm CS}$ is the reconstructed image, $\Psi$ is the sparsity basis.

The performance of the proposed GI scheme is good because of two reasons. On the one hand, CCNGI scheme enhances the SNR performance by using NGI technique. In traditional GI (black dashed line part, GI), the image in terms of $T(x,y)$ is obtained by the second-order correlation function of the intensity fluctuations of two detectors

$$\begin{aligned} T_{\rm GI}(x,y) &= \langle O(x,y)_{\rm GI}\rangle \\ &= \frac{1}{M}\sum_{i=1}^{M}(S_i - \langle S\rangle)(I_i(x,y) - \langle I(x,y)\rangle) \\ &= \langle SI(x,y)\rangle - \langle S\rangle\langle I(x,y)\rangle, \end{aligned} \tag{5}$$

the contribution to the reconstruction for each iteration $i$ is

$$O_i(x,y) = (S_i - \langle S\rangle)(I_i(x,y) - \langle I(x,y)\rangle), \tag{6}$$

where $\langle\cdot\rangle = \sum_i/M$ means an ensemble average for $M$ iterations, and the final reconstruction is obtained by averaging over all the iterations

$$T_{\rm GI}(x,y) = \langle O(x,y)_{\rm GI}\rangle. \tag{7}$$

There exists another iterative algorithm which normalizes each individual measurement $S_i$, as well as the running average instead, according to the reference signal $R_i$, resulting in an arguably more intuitive approach for dealing with time varying noise source in NGI technique. The algorithm used to describe each contribution to the reconstruction now is changed to

$$O_i(x,y) = \left(\frac{S_i}{R_i} - \frac{\langle S_i\rangle}{\langle R_i\rangle}\right)(I_i(x,y) - \langle I(x,y)\rangle), \tag{8}$$

where $\langle S_i\rangle/\langle R_i\rangle \approx \langle S_i/R_i\rangle$ is assumed for a large number of measurements. If the objects are not pure phase objects, the difference between the NGI and GI by the SNR performance can be expressed as[16]

$$\frac{{\rm SNR}_{\rm NGI}}{{\rm SNR}_{\rm GI}} = 1 + \frac{\bar{T}^2}{\overline{\delta T^2}}, \tag{9}$$

where $T$ represents object transmission function, $\bar{T}$ denotes average transmission function, and $\overline{\delta T^2} = \overline{T^2} - \overline{T}^2$ indicates the variance.

On the other hand, CCNGI scheme reduces the reconstruction time by utilizing both CS and CI techniques. First, the reconstruction data with CI technique are approximately the half of that in traditional GI. CI technique presents that the target object information has already been in the reference beam, the key to effectively extract the object information in the reference beam is how to select those intensity distribution $I_i(x,y)$ to the contribution of the reconstruction. Utilizing the CI technique, only the vectors $\{I_i(x,y)^+\}$, which correspond to $\{S_i^+\}$, are chosen for the contribution to reconstruction in the reference beam. Here, $S_i^+$ is the measurement value being greater than the average $\langle S\rangle$ in the signal beam. Normally, the number of the vectors $\{I_i(x,y)^+\}$ is approximately the half of that of the vectors $\{I_i(x,y)\}$ in traditional GI scheme. Secondly, the images in CCNGI scheme are reconstructed using the recovery algorithm of CS technique. The main idea behind CS technique is to exploit the redundancy in the structure of most natural signals/objects to reduce the number of measurements required for faithful reconstruction. Hence, the proposed GI scheme with CS technique will have higher imaging efficiency and resolution.

## 3. Numerical simulations

To verify the performance of the CCNGI scheme, we present some numerical simulations in this section. In order to illustrate the performance of CCNGI objectively, we use mean square error (MSE) and peak signal-to-noise ratio (PSNR) to calculate the degree of deviation between the reconstructed image and the original image. For an $M \times N$ size of image, MSE and PSNR are defined as[39]

$${\rm MSE} = \frac{\sum_{0\le i<M}\sum_{0\le j<N}(X_{i,j} - X'_{i,j})^2}{M\times N}, \tag{10}$$

$${\rm PSNR} = 10\lg\frac{X_{\rm max}^2}{\rm MSE}\quad ({\rm dB}), \tag{11}$$

where $X_{i,j}$ and $X'_{i,j}$ represent the original and the reconstructed images, respectively, $X_{\rm max}$ is the maximum possible pixel value of the image. Generally, the higher the PSNR is, the better quality the reconstructed image has.

In the numerical simulations, the pseudo-thermal source is generated by a Gaussian beam with wavelength $\lambda = 633$ nm under Fresnel–Huygens diffraction. The size of the images is $64\times 64$ pixels. Orthogonal matching pursuit (OMP) algorithm is used as the reconstruction algorithm, and DCT is selected as the sparsity basis in the CS technique. Since the measurement matrix is too big to operate in the laptop computer, we divide the original image to 4 blocks and use the CCNGI scheme to reconstruct the $32\times 32$ pixels blocks individually. The laptop is AMD Athlon(tm) P320 with 2.09 GHz dual-CPU and 2 GB memory.

The numerical simulations are taken for the different grayscale objects with GI scheme, NGI scheme, GISC scheme, and CCNGI scheme, respectively in Fig. 2, where figure 2(a) is for the two-grayscale "double-slit", figure 2(b) is for a two-grayscale character "NUPT", and figure 2(c) is for an eight-grayscale "Lena" object. The number of measurements using GI scheme and NGI scheme is set up to 5000, and the number of measurements using CCNGI and GISC is 2500. The direct evaluations for the imaging show that the quality of reconstructed images using the CCNGI scheme are superior to those using the NGI or GI schemes and are almost the same as the results obtained using the GISC scheme. At the same time, the PSNR values with the CCNGI scheme are much higher than those with the GI and NGI scheme with a half measurements number. Although the quality and the measurements number using the CCNGI and GISC schemes are almost the same, the measurement data for the reconstruction using CCNGI is half of that of GISC scheme for applying CI technique.

Because of the randomness of pseudo-thermal intensity distribution in numerical simulations, we present the average MSE and PSNR values of the reconstructed image using GI, NGI, and CCNGI schemes over 10 times in Tables 1 and 2, respectively. It is shown that the qualities of the images using CCNGI have been improved greatly with the half of measurements. For the "NUPT" character object, the average MSE over 10 times for the CCNGI scheme was 0.059, which has been reduced to 28.095% of that using the traditional GI scheme, and has been reduced to 39.597% of that using the NGI scheme. The results from Table 2 also verify that the CCNGI scheme has improved the qualities of the reconstructed images in comparison with those from the traditional GI scheme and the NGI scheme.

Figure 3 further shows the MSE curve against the different measurement numbers using GI, NGI, GISC, and CCNGI schemes for the double-slit object. As it can be seen from the figure, the MSE flattens out for $M > 1800$ (43.9% for the Nyquist limit of $64 \times 64$) with values of 0.03. The result also shows that the MSE value obtained using CCNGI scheme is lower than those found using NGI and GI schemes from 0 to 5000 measurements, and is almost the same as that using the GISC scheme in the correlated imaging system. We further compare the reconstruction time for the CCNGI scheme and the GISC scheme in Fig. 4. The result shows that the reconstruction time using CCNGI is much shorter than that using the GISC scheme from 0 to 5000 measurements.

**Table 1.** Results of the average MSE.

| | Double-slit | NUPT | Lena |
|---|---|---|---|
| GI | 0.237 | 0.210 | 0.089 |
| NGI | 0.164 | 0.149 | 0.049 |
| CCNGI | 0.021 | 0.059 | 0.024 |
| NGI decrease percent (GI) | 30.802% | 29.048% | 44.944% |
| CCNGI decrease percent (GI) | 91.139% | 71.905% | 73.034% |
| CCNGI decrease percent (NGI) | 87.195% | 60.403% | 51.02% |

**Table 2.** Results of the average PSNR values.

| | Double-slit | NUPT | Lena |
|---|---|---|---|
| GI | 6.253 | 6.778 | 10.506 |
| NGI | 7.852 | 8.268 | 13.098 |
| CCNGI | 16.579 | 12.256 | 16.198 |
| NGI increase percent (GI) | 25.572% | 21.983% | 24.672% |
| CCNGI increase percent (GI) | 165.137% | 80.820% | 54.179% |
| CCNGI increase percent (NGI) | 111.144% | 48.234% | 23.668% |

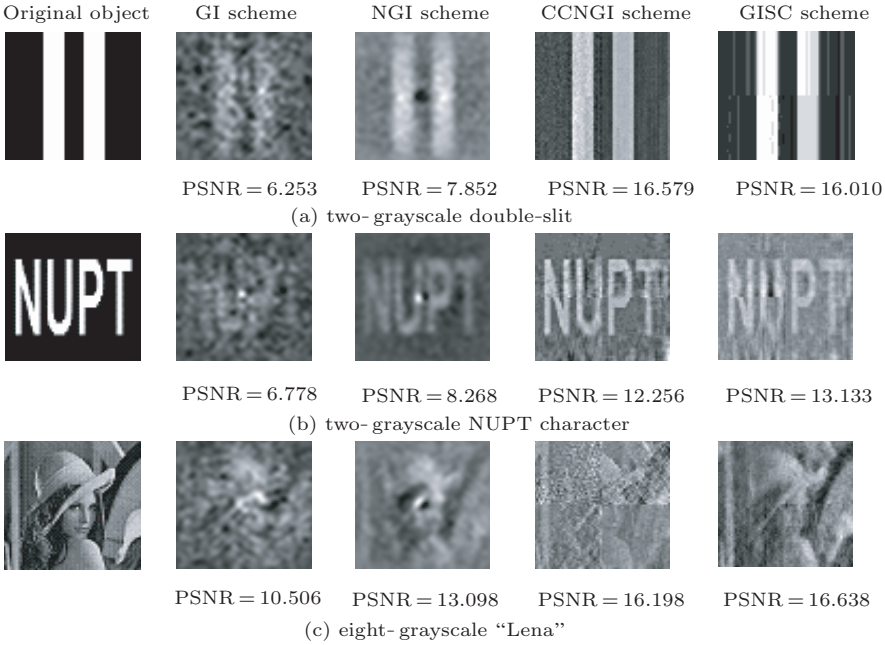



**Fig. 2.** (color online) Comparison of the images from GI, NGI, and CCNGI schemes for different grayscale objects: (a) two-grayscale double-slit, (b) two-grayscale NUPT character, and (c) eight-grayscale "Lena".

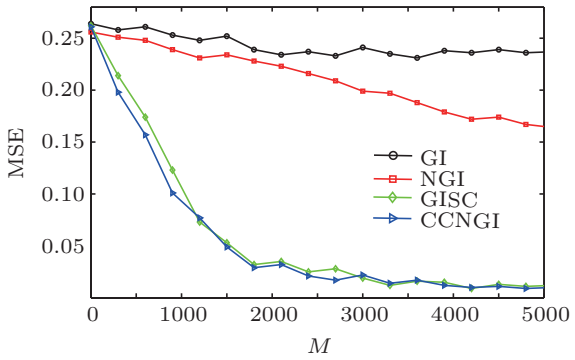



**Fig. 3.** (color online) Calculated mean square error (MSE) of the reconstructed correlated imaging of "double-slit"as a function of the number of measurements $M$.

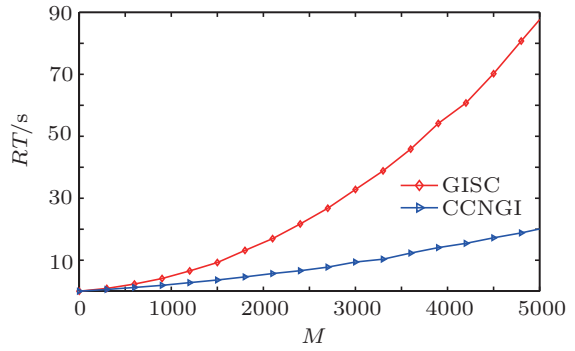



**Fig. 4.** (color online) The reconstruction time (RT) for correlated imaging of "double-slit" as a function of the number of measurements $M$.

## 4. Conclusion

In the paper, we have proposed a CCNGI scheme with a short reconstruction time and good MSE performance. We have enhanced the SNR performance of the GI system by normalizing the reference beam intensity to eliminate the noise caused by laser power fluctuations, and have reduced the reconstruction time by using both CS and CI techniques. The numerical simulation results show that the qualities of reconstructed images using the CCNGI scheme are better than those using NGI and GI schemes, and the number of measurements has decreased greatly. With the 64×64 pixels image, the MSE value tends to be stable when the measurement numbers is 1800. We also find that the double-slit object's MSE by GI and NGI schemes are 0.237, 0.164 respectively with 5000 measurement numbers, and the MSE by CCNGI scheme is 0.021 with only 2500 measurement numbers. The CCNGI scheme has better imaging quality and a less reconstructing time in comparison with GI and NGI schemes. The results show that for the "Lena" image object, the average MSE over 10 times for CCNGI scheme has been reduced 73.034% as compared to the result using the GI scheme, and has been reduced 51.02% as compared to the result using NGI scheme. In addition, the qualities of the reconstructed images using CCNGI are almost the same as those using the GISC scheme with a shorter reconstruction time.

## References

[1] Klyshko D N 1988 *Photons and Nonlinear Optics* (New York: Gordon and Breach Science)
[2] Pittman T B, Shih Y H, Strekalov D V and Sergienko A V 1995 *Phys. Rev. A* **52** R3429
[3] Strekalov D V, Sergienko A V, Klyshko D N and Shih Y H 1995 *Phys. Rev. Lett.* **74** 3600
[4] Abouraddy A F, Saleh B E A, Sergienko A V and Teich M C 2001 *Phys. Rev. Lett.* **87** 123602
[5] Zhao S M, Ding J, Dong X L and Zheng B Y 2011 *Chin. Phys. Lett.* **28** 124207
[6] Zhao S M,Yang H, Li Y Q, Cao F, Sheng Y B, Cheng W W and Gong L Y 2013 *Opt. Commun.* **294** 223
[7] Li Y Q, Yang H, Liu J, Gong L Y, Sheng Y B, Cheng W W and Zhao S M 2013 *Chin. Opt. Lett.* **11** 021104
[8] Bennink R S, Benley S J and Boyd R W 2002 *Phys. Rev. Lett.* **89** 113601
[9] Gatti A, Brambilla E, Bache M and Lugiato L A 2004 *Phys. Rev. A* **70** 013802
[10] Valencia A, Scarcelli G D, Angelo M and Shih Y H 2005 *Phys. Rev. Lett.* **94** 063601
[11] Li H, Chen Z, Xiong J and Zeng G H 2012 *Opt. Express* **20** 2956
[12] Li H, Xiong J and Zeng G H 2011 *Opt. Eng.* **50** 127005
[13] Shapiro J H 2008 *Phys. Rev. A* **78** 061802
[14] Gong W L and Han S S 2010 *Phys. Lett. A* **374** 1005
[15] Ferri F, Magatti D, Lugiato L A and Gatti A 2010 *Phys. Rev. Lett.* **104** 253603
[16] Sun B Q, Welsh S S, Edgar M P, Shapiro J H and Padgett M J 2012 *Opt. Express* **20** 16892
[17] Gong W L and Han S S 2012 *Phys. Lett. A* **376** 1519
[18] Katz O, Bromberg Y and Silberberg Y 2009 *Appl. Phys. Lett.* **95** 131110
[19] Wang H and Han S S 2012 *Europhys. Lett.* **98** 24003
[20] Zhao C Q, Gong W L, Chen M L, Li E R, Wang H, Xu W D and Han S S 2013 *Appl. Phys. Lett.* **101** 141123
[21] Gong W L and Han S S 2012 *Phys. Lett. A* **376** 1519
[22] Du J, Gong W L and Han S S 2012 *Opt. Lett.* **37** 1067
[23] Gong W L and Han S S 2012 *J. Opt. Soc. Am. A* **29** 1571
[24] Gong W L and Han S S 2013 *Appl. Phys. Lett.* **102** 021111
[25] Bai X, Li Y Q and Zhao S M 2013 *Acta Phys. Sin.* **62** 044209 (in Chinese)
[26] Luo K H, Huang B Q, Zheng W M and Wu L A 2012 *Chin. Phys. Lett.* **29** 074216
[27] Li M F, ZhangY R, Luo K H, Wu L A and Fan H 2013 *Phys. Rev. A* **87** 033813
[28] Wen J M 2013 *J. Opt. Soc. Am. A* **29** 1906
[29] Bai Y F, Yang W X and Yu X Q 2012 *Chin. Phys. B* **21** 044206
[30] Liu Q, Luo K H, Chen X H and Wu L A 2010 *Chin. Phys. B* **19** 094211
[31] Katkovnik V and Astola J 2012 *J. Opt. Soc. Am. A* **29** 1556
[32] Meyers R E, Deacon K S and Shih Y H 2012 *Appl. Phys. Lett.* **100** 131114
[33] Hardy N D and Shapiro J H 2013 *Phys. Rev. A* **87** 023820
[34] Chen W and Chen X D 2013 *Opt. Lett.* **38** 546
[35] Zhang E F and Dai H Y 2011 *Acta Phys. Sin.* **60** 064209 (in Chinese)
[36] Yang H and Zhao S M 2012 *Acta Opt. Sin.* **32** 243 (in Chinese)
[37] Donoho D L 2006 *IEEE Trans. Infor.* **52** 1289
[38] Candes E J and Wakin M B 2008 *IEEE Signal Process. Mag.* **25** 21, and refrences therein
[39] Koschan A and Abidi M 2008 *Digital Color Image Processing* (New Jersey: Wiley-Interscience)